Inhibition of Chymotrypsin by a Complex of Ortho-Vanadate and Benzohydroxamic Acid: Structure of the Inert Complex and Its Mechanistic Interpretation[†]

Aaron Moulin,[‡] Jason H. Bell,[§] R. F. Pratt,[*,§] and Dagmar Ringe[*,‡]

Rosenstiel Basic Medical Sciences Research Center, Program in Biochemistry, and Program in Biophysics, Brandeis University, Waltham, Massachusetts 02454, and Department of Chemistry, Wesleyan University, Middletown, Connecticut 06459

ABSTRACT: Serine proteases, like serine β-lactamases, are rapidly and covalently inhibited by suitably designed phosph(on)ates. The active sites of these enzymes must, therefore, be able to stabilize the pentacoordinated transition states of phosphyl transfer reactions as well as the tetrahedral transition states of acyl transfers. It follows that these enzymes should also be inhibited by molecules capable of generating inert pentacoordinated species. We (J.H.B. and R.F.P.) have previously shown that these enzymes are, in fact, rapidly and reversibly inhibited by 1:1 complexes of vanadate and hydroxamic acids. In this paper, we present the first crystal structure of an acyl transferase inhibited by vanadate. The complex of vanadate and benzohydroxamic acid is a competitive inhibitor of α-chymotrypsin with a K_I value of 16 μM. In the structure, obtained at a resolution of 1.5 Å, the protein is conformationally little different from the apoenzyme. The vanadium, in a distorted octahedral ligand field, is covalently bound to the active site serine oxygen group. One oxgen ligand, presumably anionic, is located in the oxyanion hole. Another is directed roughly in the direction of the acyl transfer leaving group, and a third in the direction of the S2 site. The hydroxamate is bound to vanadium through the hydroxyl oxygen and also, more weakly, through the carbonyl group, to form a five-membered chelate ring. The effect of this chelation is to place the phenyl group of the inhibitor into the important S1 specificity site. The hydroxamate oxygen is directed in line away from the Ser195 Oγ, approximating the direction of departure of a leaving group in phosphyl transfer. The entire complex can be seen as a reasonable mimic of a phosphyl transfer transition state where the leaving group is extended into the S1 site.

The study of enzymes has regularly been informed by the discovery of new inhibitors. With respect to insight into events at the active site of enzymes, related to catalysis, the most informative inhibitors have generally been substrate or product analogues (*1*), transition state analogues (*2–4*), or of the mechanism-based variety (*5–8*). Depending, to a considerable degree, on the nature of the mechanism of catalysis employed by the enzyme concerned and on the class of inhibitor, the final complex may contain the inhibitor either covalently or noncovalently attached to the enzyme. In general, inhibitors that must undergo covalent reaction to achieve the final complex may reach that state by way of transition states that differ in structure, i.e., in geometry and/ or charge distribution, from those of the normal enzyme-catalyzed reaction. If such reactions are unusually rapid, however, as would be expected to occur in the case of a particularly effective inhibitor, then the enzyme active site must be able to stabilize the transition state of the reaction leading to inhibition. It follows, therefore, that a new class of inhibitor could be achieved from a stable analogue of this latter transition state. This situation is shown diagrammati-
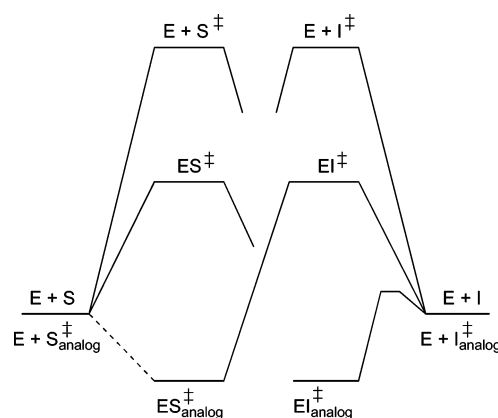

FIGURE 1.

cally in the free energy/reaction coordinate diagram of Figure 1 where a good transition state analogue of the enzyme-catalyzed reaction (ES$^{\ddagger}_{analogue}$) cannot be achieved by a simple noncovalent binding reaction, but only by way of a covalent reaction between E and I that passes through a transition state EI‡, and one that is, in the present example, significantly stabilized by the enzyme (compare the energies of E+I‡ and EI‡).[1] Under these circumstances, EI$^{\ddagger}_{analogue}$, a stable analogue

* Corresponding authors. R.F.P.: tel, 860-685-2629; e-mail, rpratt@ wesleyan.edu; fax, 860-685-2211. D.R.: e-mail, ringe@brandeis.edu.
[‡] Brandeis University.
[§] Wesleyan University.

[1] Abbreviations: DMSO, dimethyl sulfoxide; EI, enzyme–inhibitor complex; ES, enzyme–substrate complex; MPD, 2-methyl-2,4-pentanediol; NMR, nuclear magnetic resonance; PEG, polyethylene glycol.

of EI‡, and possibly significantly different in structure from ES‡, should also be an effective inhibitor.

Serine proteases have been a traditional testing ground for enzyme inhibitors and, in particular, of transition state analogue inhibitors. The central distinguishing feature of an acyl transfer reaction, such as catalyzed by serine proteases, is the anionic tetrahedral intermediate and associated transition states (*9*). Since serine proteases operate by a double displacement mechanism with a covalent acyl−enzyme intermediate (*10*), the tetrahedral intermediates of acylation (**1**: L denotes a leaving group) and deacylation (**2**) are covalently bound to the active site serine nucleophile.
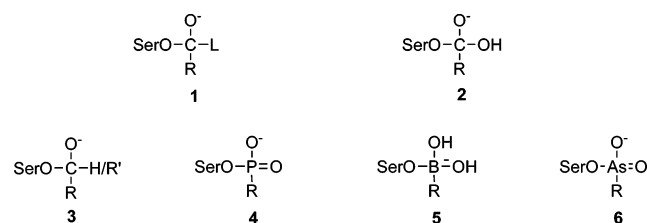
Transition state analogue inhibitors, therefore, typically take the form of tetrahedral anions covalently bound to the active site serine. Examples are carbonyl adducts, **3**, phosphonates, **4**, boronates, **5**, and arsonates, **6**. In each of these instances, crystal structures have shown the inhibitors placed at the active site in a conformation that rationally mimics a tetrahedral intermediate of the enzyme-catalyzed reaction (*11*).

The inhibition of serine proteases by phosphyl derivatives has been studied for many years (*12*) and, with suitably specific inhibitors, is a very rapid reaction (*13−15*). It is clear, therefore, that the enzyme active site must actively catalyze this reaction. The transition state of a phosphylation reaction contains pentacoordinated phosphorus and is thought to have a trigonal bipyramidal geometry (*16*). The enzyme, therefore, must be able to bind and stabilize a species such as **7** and **8**, as well as the classical **1−6** (*17*). From the
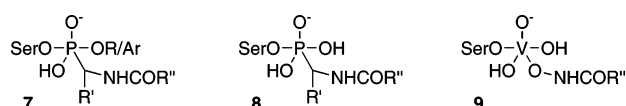
arguments made above (Figure 1), a stable pentacoordinated structure, bound to the enzyme, should also be an inhibitor. Stable pentacoordinated structures are not common, but among compounds of biocompatible elements, those of vanadium stand out. Vanadates have long been employed as transition state analogue inhibitors of enzymes catalyzing phosphyl transfer reactions (*18−21*). Crystal structures of the inhibitory complexes indeed reveal pentacoordinated vanadium (*22−25*).

In view of the above, therefore, we (J.H.B. and R.F.P.) looked for inhibition of α-chymotrypsin by complexes of hydroxamic acids with vanadate, anticipating that complexes of structure **9**, analogous to **8**, might be formed. We indeed did find inhibition (*26*), just as we did with another serine protease, elastase, and with a different class of serine hydrolase, the class C β-lactamases (*27*), but in no case, until now, was the structure of the inert complex determined. In this paper, we report the 1.5 Å crystal structure of chymotrypsin in complex with vanadate and benzohydroxamic acid.

The structure reveals the inhibitor at the active site and a novel mode of inhibition.

EXPERIMENTAL PROCEDURES

Materials. Bovine pancreatic α-chymotrypsin was obtained from Sigma (Type II). Benzohydroxamic acid and sodium ortho-vanadate (99.99%) were purchased from Aldrich. These reagents were used as supplied. Stock solutions of vanadate and benzohydroxamic acid for the kinetics experiments were prepared as described previously (*28*). Fresh stock solutions of α-chymotrypsin (1 mg/mL) were prepared in 1 mM hydrochloric acid immediately prior to use and kept on ice for the duration of the experiment.

Kinetics. Steady-state kinetics experiments were performed at 25 °C in 0.1 M Tris buffer at pH 7.8 containing 10 mM calcium chloride. The substrate employed was *N*-succinyl-alanyl-alanyl-prolyl-phenylalanyl-*p*-nitroanilide (Sigma); its hydrolysis, catalyzed by the enzyme, was monitored spectrophotometrically at 410 nm. The K_m of the substrate under these conditions was taken to be 43 μM (*29*). Inhibition of the enzyme (final concentration 0.2 μM) by the vanadate/benzohydroxamic acid complex was demonstrated by measurement of initial rates of substrate hydrolysis (final substrate concentration 86 μM) at constant total vanadate concentration (0.3 mM) and various hydroxamic acid concentrations (0−1 mM). The inhibition constant of the 1:1 complex was determined from these data, as previously described (*27*), employing the program Dynafit (*30*). The nature of the inhibition was demonstrated by experiments where initial rates of substrate hydrolysis were measured at fixed vanadate and hydroxamic acid concentrations but with variation of substrate concentration (5−172 μM). This procedure was repeated at different combinations of vanadate and benzohydroxamic acid concentrations, with both in the range of 0.03−1 mM. These data were analyzed by the method of Cleland (*31*). The inhibition caused by the vanadate complex was quantitatively very similar at pH 7.0 to that at pH 7.8.

Crystallization of γ-Chymotrypsin. γ-Chymotrypsin was purchased from Sigma (C-4754) as an essentially salt-free lyophilized powder. The desired amount of enzyme was dissolved in distilled deionized water to a concentration of 30 mg/mL and the solution stored at 4 °C until needed. γ-Chymotrypsin and α-chymotrypsin are conformational isomers that are identical in amino acid sequence and solution kinetics (*32*) but have different crystal structures, largely brought about by the presence of a peptide from proteolysis bound at the active site of the former (*33*).

Crystals were grown by the hanging drop vapor diffusion method. Drops consisted of a mixture of enzyme solution, buffer (10 mM sodium cacodylate pH 6.0, 0.75% saturated cetyltrimethylammonium bromide, and 45% saturated ammonium sulfate), and 1 M NaI solution. These were mixed in the ratio protein:buffer:NaI = 5 μL:4 μL:1 μL. First, the enzyme solution was pipeted onto a glass cover slip, then the buffer solution was added, and finally the NaI solution was added. The order in which the solutions were added seemed to have a distinct effect on the quality and number of crystals. The resulting 10 μL drop was not mixed mechanically but allowed to self-mix by simple diffusion, as mixing also seemed to reduce the number and size of crystals.

The above procedure produced the most crystals of highest quality. The well was filled with 700 μL of buffer solution.

Crystals were routinely grown in about 3 days by this method with dimensions of approximately $0.5 \times 0.3 \times 0.2$ mm. The crystals were tetragonal and belonged to symmetry space group $P4_22_12$, $a = b = 68.0$ Å and $c = 95.9$ Å. Crystals could be stored in the drops for months with no apparent loss of diffraction quality.

Inhibition of Crystals with the Vandate/Benzohydroxamic Acid Complex. Sodium ortho-vanadate was dissolved in water to a final concentration of 1 M. The benzohydroxamic acid was dissolved in DMSO to a final concentration of 1 M. These stock solutions were used to make a final solution of 1 mM vanadate and 2 mM benzohydroxamic acid in 20 mM sodium cacodylate (pH 7.4) and 75% saturated ammonium sulfate. These concentrations of vanadate and benzohydrox-amic acid were used since they gave the maximal concentration of the 1:1 vanadate/benzohydroxamic acid complex [higher concentrations result in the formation of noninhibitory 1:2 complexes (*27*)]. The pH was necessarily kept near neutrality to avoid formation of decavanadate at acidic pH levels.

Crystals of γ-chymotrypsin were placed in 10 μL of soaking solution for anywhere from 1 to 5 days. After 1 day of soaking, the crystals turned a characteristic reddish-brown color and appeared opaque. This is interpreted to be due to localization of vanadate/hydroxamic acid complexes in the solvent channels of the crystal. This was encouraging as it suggested that the inhibitor was able to diffuse freely through the crystal. Crystals could be left in the soaking solution for several weeks without evidence of dissolution of crystals. Backsoaking of crystals in 20 mM sodium cacodylate (pH 7.4) and 75% ammonium sulfate lacking inhibitor resulted in loss of the reddish-brown color and opaqueness. This indicates that the vanadate compounds can always diffuse freely through the crystal.

Data Collection and Reduction. For crystals soaked in high ammonium sulfate concentration, a cryo solution of 22% PEG 4K and 15% MPD in water was prepared. Crystals were passed through this solution transiently and then flash cooled in liquid nitrogen. Data were collected at the Advanced Photon Source at Argonne National Laboratories on Bio-CARS beamline 14-BM-C to a final resolution of 1.5 Å. Exposure times were 5.0 s with an incident wavelength of 1.00 Å and an oscillation sweep of 0.5°. The data were indexed and integrated using DENZO and scaled using SCALEPACK (*34*). The resulting scaled data had an overall R_{merge} of 7.4%. A summary of data statistics is given in Table 1.

CNS Refinement. These data were initially refined in CNS (*35*). Phases were derived from a starting model taken from the Brookhaven Protein Data Bank, call number 2GCH (*36*). The refinement was carried out with a maximum likelihood amplitude-based target function, employing chemical re-straints (*37*). R_{free} was used as a monitor of refinement. No inhibitor or waters were included in the initial refinement. See Table 1 for further information.

The starting model was first subjected to rigid body refinement. The resulting model was optimized by one round of simulated annealing torsion angle refinement (*38*). The model was further improved with one round each of both group and individual isotropic B-factor refinement as imple-

Table 1: Data Collection and Refinement Statistics

Crystal Data	
space group	$P4_22_12$
unit cell parameters (Å)	$a = 69.0$
	$b = 69.0$
	$c = 95.9$
Data Processing	
no. of reflections, observed	1 054 360
no. of reflections, unique	38 061
cutoff (I/σ)	0
$R_{merge}{}^a$ (overall) (%)	7.4
completeness, overall (%)	98.9
highest resolution shell (Å)	1.55−1.50
$R_{merge}{}^a$ (outer shell) (%)	46
completeness, outer shell (%)	94.8
Model Refinement	
resolution range (Å)	50−1.5
cutoff ($F/\sigma F$)	0
R-factor^b (%)	20.0
no. of reflections	63183
R_{free} (for 2053 reflections; %)	24.3
no. of protein atoms	3290
no. of vanadium ions	1
no. of sodium ions	1
no. of sulfate ions	1
no. of water molecules	276
no. of other non-protein atoms	13
B factor model	individual
rmsd from ideality:	
bond lengths (Å)	0.007
bond angles (deg)	1.7
improper angles (deg)	1.0
dihedral angles (deg)	22.7

^{a} $R_{merge} = \sum |I_{obs} - I_{avg}|/\sum I_{avg}$. ^{b} R-factor $= \sum |F_{obs} - F_{calc}|/\sum |F_{obs}|$.

mented in CNS. Throughout this process, model quality was also checked manually in O (*39*) against electron density maps with coefficients $F_o - F_c$ and $2F_o - F_c$. Maps drawn at this stage in the refinement showed clear and unambiguous difference density for the inhibitor in the active site. Maps also showed little need to adjust the overall protein model, as it fitted quite well into the observable density. No solvent molecules were added in CNS. After the individual B-factor refinement, $R = 26.9\%$ and $R_{free} = 27.3\%$ and included 236 amino acid residues (residues 1−10, 16−146, and 151−245; residues 14−15 and 147−148 are cleaved during zymogen activation and residues 11−13, 149, and 150 are disordered). Subsequently, all refinement was carried out in SHELX-97-2 (*40*).

SHELX-97 Refinement. The CNS model was refined in SHELX using a conjugate gradient least-squares minimiza-tion against an intensity based residual target function. Stereochemical and displacement parameters were used. Waters were added after one round of refinement. After another round of refinement with waters, the inhibitor was added. A coordinate file for the inhibitor was generated by ChemDraw and WebViewer Lite. Refinement parameters were derived for SHELX from CSD coordinate file KEFNUE.pdb (*41*). More waters were added on subsequent rounds, generally 50 at a time. Between all rounds of refinement, adjustments in the protein model and solvent model were made by hand in O. Upon addition of more waters, difference density for alternate conformations ap-peared in both the protein and the inhibitor. It should also be noted that there are significant regions of connected difference density in solvent accessible regions, especially
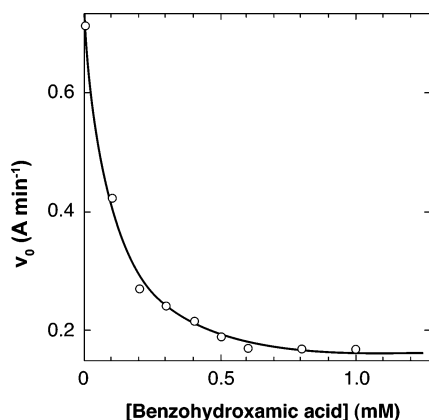
FIGURE 2: Inhibition of turnover of *N*-succinyl-alanyl−alanyl-prolyl-phenylalanyl-*p*-nitroanilide by α-chymotrypsin in the presence of 0.3 mM total vanadate and 0−1 mM benzohydroxamic acid.

FIGURE 3: Double-reciprocal plots of the activity of α-chymotrypsin against *N*-succinyl-alanyl−alanyl-prolyl-phenylalanyl-*p*-nitroanilide in the absence of vanadate and benzohydroxamic acid (○), in the presence of 0.1 mM total vanadate and 0.03 mM benzohydroxamic acid (□), and of 0.1 mM total vanadate and 0.1 mM benzohydroxamic acid (△). These plots show the inhibition by vanadate and benzohydroxamic acid to be competitive.

Scheme 1

near the active site, that appear to be portions of peptide density. These are most likely self-cleavage products, as it is known that γ-chymotrypsin cleaves itself during formation of crystals. These regions of difference density were not modeled as resolution precluded definite identification of sequence and inclusion of a poly-alanine model (three residues) did not significantly improve either R or R_{free}. In addition to the inhibitor molecule, a sulfate molecule was modeled. At the end of SHELX-97 refinement, the final R = 20.0% and R_{free} = 24.3%. A summary of final refinement statistics is given in Table 1. Coordinates and structure factors have been deposited in the RCSB Protein Data Bank as entry 2P8O.

RESULTS

Hydroxamic acids form coordination complexes with vanadate at neutral pH. At concentrations below millimolar, 1:1 complexes dominate (*28*). Such a mixture of benzohydroxamic acid and vanadate inhibited α-chymotrypsin in a fast and reversible fashion (Figure 2). Neither the hydroxamic acid nor vanadate alone affected the enzyme activity at these concentrations. The data of Figure 3 show that the inhibition was of the competitive type; this was also true at 1 mM vanadate (data not shown). Analysis of the data of Figure 3 was performed by means of the previously employed (*27*) Scheme 1. In this scheme, VH and VH_2 represent the 1:1 and 1:2 vanadate−hydroxamic acid complexes, V_2 and V_4 are divanadate and tetravanadate, respectively, EVH is the inhibitory complex, and S is the peptide substrate turned over by the enzyme E to product P. It is also assumed that the inhibitor is the 1:1 VH complex. This was proven to be true for a serine β-lactamase (*27*) and is confirmed in the present case by the structure obtained (see below). The constants $K_1−K_4$ were independently determined as previously described (*27, 28*), and thus K_I could be obtained from the data of Figures 2 and 3.

The K_I value for the benzohydroxamic acid/vanadate complex was (14 ± 1) μM. Values for the vanadate complexes of *p*-nitro- and *p*-methoxy-benzohydroxamic acids (data not shown) were (6.0 ± 0.5) μM and (38 ± 1) μM. The electrophilicity of vanadium, increased by electron withdrawing substituents on the benzohydroxamate ligand, may therefore be important in enhancing the inhibitory power
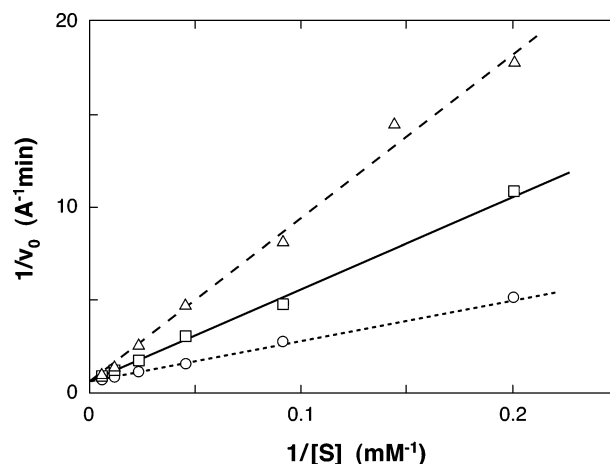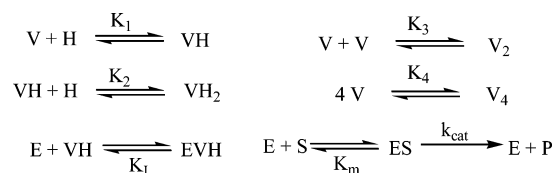
of the vanadate complex. A ^{51}V NMR spectrum of the vanadate/benzohydroxamic acid/chymotrypsin ternary complex [a mixture of 1 mM total vanadate, 2 mM benzohydroxamic acid, and 1 mM α-chymotrypsin was prepared at pH 7.5 and its NMR spectrum obtained as described previously (*27*)] (not shown) exhibited sharp peaks for vanadate monomer (−559 ppm) and the free VH complex (−509 ppm) and a broad resonance around −500 ppm which can be assigned to the E·VH complex. A similar resonance (−498 ppm) in the analogous complex of the *Enterobacter cloacae* P99 β-lactamase was interpreted to indicate the presence of 5- or 6-coordinated vanadium in the complex (*27*). This, too, is in accord with the structure described below.

Overall Structure. The overall fold and crystal packing of the enzyme is identical to that of previous structures of γ-chymotrypsin. Solvent boundaries are well defined and all regions of protein density are clear except for residues 11, 12, 13, 149, and 150, which are traditionally disordered in γ-chymotrypsin structures (*32, 42*). Areas near the trypsin and chymotrypsin cleavage sites display weak density, particularly the area near residues 145 and 146 where placement of arginine 145 was not possible.

At the high resolution achieved, there seems to be evidence of only minimal decarboxylation of aspartate and glutamate side chains on the surface of the protein, a phenomenon characteristic of synchrotron radiation. There is also significant difference density (>2.5 σ) around certain internal β strands (e.g., residues 211−214), consistent with small displacement of the peptide backbone. There is little or no corresponding difference electron density for the side chains. Modeling of the backbone into the difference electron density followed by energy minimization refinement yielded electron density maps with significant difference electron density
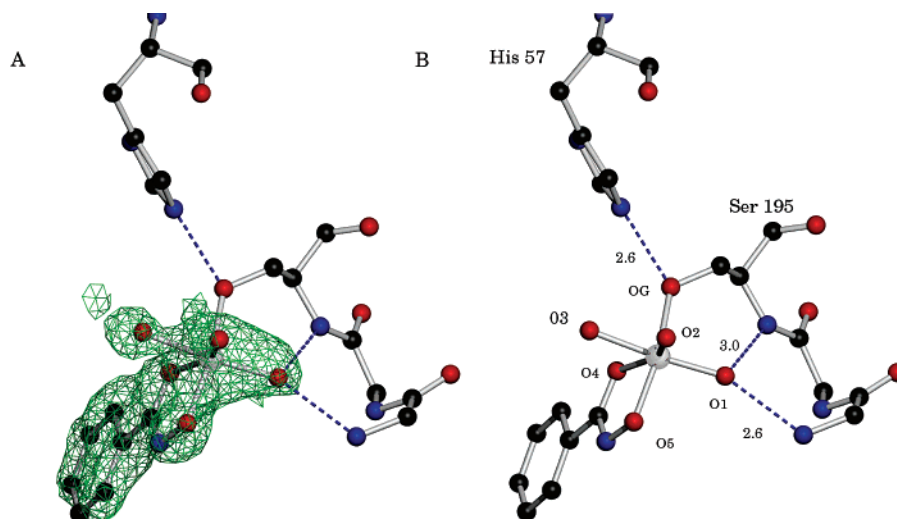
FIGURE 4: Two-paneled figure of the active site showing the vanadate/benzohydroxamic acid complex covalently attached to γ-chymotrypsin. In panel A, the initial difference electron density (coefficients $F_o - F_c$) before refinement of the inhibitor in SHELX is shown in green, rendered at 2.5 σ. Panel B shows the electron density removed and with appropriate labels added. The vanadium ion is rendered in chrome, and the oxygens are numbered as in the text. The residues of the oxyanion hole are also shown with pertinent distances in angstroms. Only the side chains of His 57 and Ser 195 are rendered.

corresponding to the former position of the backbone. This seems to indicate that these β strands have alternate positions in the crystal. Due to concerns with resolution, these alternate positions were not modeled. All the disulfide bonds present in the protein have nearby residual difference electron density. This would indicate that there is some degree of reduction of the disulfides, probably X-ray induced. The greatest degree of reaction seems to have occurred at the Cys 42–Cys 58 disulfide bond, which is proximal to the active site. It is possible that vanadium might facilitate redox reactions at sulfur. A sulfate molecule resides in a part of the solvent-accessible regions of the crystal making hydrogen-bonding contacts with the backbone amide nitrogen of serine 92 and the Nζ of lysine 36 of a symmetry related protein molecule as well as nearby water molecules.

The Active Site. The active site region is well defined and has a conformation similar to the active sites of other chymotrypsin–inhibitor complexes. Initial maps drawn using the atomic coordinates from Cohen et al. (*36*) showed clear difference electron density in the active site for the vanadium/ hydroxamate adduct. The inhibitor is bound covalently to the vanadium ion through a covalent bond with Ser 195Oγ (Figure 4). The aromatic ring of the benzohydroxamic acid moiety points into the hydrophobic S1 pocket of the enzyme. The initial difference electron density indicated an octahedral geometry about the vanadium atom with the carbonyl and hydroxyl of the benzohydroxamic acid, the Ser 195Oγ and three other oxo ligands all coordinating to the vanadium center (see the schematic Figure 5). Of the three oxo ligands, ligand O1 is oriented into the oxyanion hole and makes hydrogen bonds with backbone amide nitrogens of residues 195 and 193. Ligands O2 and O3 point out toward solvent and make minimal contacts with the protein.

The phenyl ring of the hydroxamate fits neatly into the S1 binding pocket. The π-cloud of the phenyl ring makes several interactions with peptide backbone. The phenyl ring is sandwiched between two β strands and the π-cloud of the ring makes a stacking-type interaction with the delocalized π electrons in the peptide bonds of the protein backbone. The phenyl ring extends only part way into the pocket, not
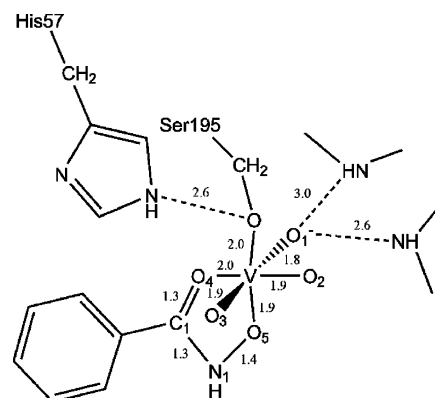

FIGURE 5: A chemical representation of the structure shown in Figure 4 with pertinent distances in angstroms. The protonation states of the oxygen species are not indicated, as definite knowledge of the protonation states cannot be determined at this resolution. The oxygens are numbered as discussed in the text.

quite as far as tryptophan would, for example, with the rest of the pocket being occupied by several water molecules. The ring is slightly mobile, with some motion in the plane of the ring, judging by a slight elongation of the density on either side of the phenyl ring. There does not, however, seem to be any motion of the ring perpendicular to the plane of the ring, judging by the electron density.

The residues of the catalytic triad—Ser 195, His 57, and Asp 102—are well ordered with low B-factors. They are hydrogen bonded together in the usual fashion for serine proteases with Ser 195Oγ–His 57Nϵ2 and His 57Nδ1–Asp 102Oδ1 distances of 2.6 Å. These values are typical for acyl–enzyme and transition state analogue complexes of these enzymes and emphasize, particularly, the tight hydrogen bond between His 57 and Asp 102 that would be expected of reactive complexes and their analogues (e.g., see refs *42–44*).

Coordination around Vanadium. The coordination about the vanadium in the difference electron density is close to octahedral. Figure 5 shows the bond lengths for the vanadium/ benzohydroxamic acid ligand. The vanadium–oxygen dis-

tances are generally 1.8−2.0 Å, which agrees well with data from small molecule studies. The bond angles are also consistent with those seen in small molecule structures with most of them being within 15° of their expected ideal values. The average deviation from ideal octahedral geometry is 5.5°. The 2005 version (5.27) of the Cambridge Structural Database lists 14 structures including 17 individual hydroxamates coordinated to V^V; all are approximately octahedral complexes (*41*, *45−51*). The average distances relevant to vanadium coordination of the hydroxamate are $V−O_5$, 1.88 ± 0.03 Å; $O_5−N_1$, 1.37 ± 0.02 Å; $N_1−C_1$, 1.32 ± 0.02 Å; $C_1−O_4$, 1.25 ± 0.02 Å; and $O_4−V$, 2.15 ± 0.07 Å. These are in excellent agreement with those determined in the chymotrypsin complex. The reference compounds also contain examples of complexes of *N*-aryl hydroxamic acids which have bond lengths in the ranges noted above. This supports the assignment of the reference structures as hydroxamates rather than hydroximates. The $C_1−O_4$ and $N_1−C_1$ distances would also be longer and shorter, respectively, if the latter were true (*52*). The resolution of the present structure is insufficient to decide between hydroxamate and hydroximate, but, based on the cited precedents, the present structure was modeled as a hydroxamate.

It is noticeable that the $O_4−V$ distance appears to be somewhat shorter in the chymotrypsin complex than in the reference compounds (2.0 vs 2.15 Å). This may relate to another point. All of the reference complexes contain one oxygen ligand which is 1.59 ± 0.03 Å from the vanadium, connected to it by what is generally described as a vanadium oxygen double bond. Distribution of the double bond character among the three oxygen ligands of the chymotrypsin complex (none of the model compounds has more than one oxygen) would certainly lead to longer V−O bonds; the V−O (usually three) bond lengths reported for pentacoordinate vanadate complexes of phosphoryl transfer enzymes, for example, appear to vary rather widely from 1.5 Å to 2.0 Å. Another contributing factor to the longer V−O bonds may be the shorter $V−O_4$ distance in the complex than in the reference compounds, which may be enforced by the fit of the phenyl group in the P_1 site. The shortest V−O bond in the complex corresponds to the oxygen in the oxyanion hole. Although it is not easy to directly determine, at the resolution achieved, whether a particular oxygen exists in the structure as oxide, hydroxide, or water, it seems likely, because of the functional role of the oxyanion hole in catalysis, that O_1, at least, is anionic. The shorter bond length is perhaps not unexpected for a site that is designed to accommodate an even shorter $C−O^-$ moiety.

Another interesting feature is the apparent length of the Ser 195$O\gamma$−V bond (2.0 Å). Normally, V−OR bonds are 1.75−1.80 Å (Cambridge Structural Database), but, when protonated, for example in the structures described by Maurya et al. (*53*), the V−O bond exceeds 2.0 Å in length. With respect to the present structure, the partial protonation provided by the strong hydrogen bond donated by His 57Nϵ may be responsible for the bond extension.

After refinement of the octahedral vanadium/benzohydroxamic acid complex against the data, a small amount (≤5%) of residual difference electron density appeared between atoms O2 and O3. This was interpreted as being consistent with a small amount of a trigonal bipyramidal coordination around the vanadium center. In this putative

trigonal bipyramidal structure, the benzohydroxamic acid moiety, the vanadium center, and O1 all retain the same position as in the octahedral form, but O2 and O3 are replaced by an intermediary oxygen, giving a roughly trigonal plane around the vanadium. Refinement of only this trigonal bipyramidal form showed very poor occupancy for the intermediary oxygen position, indicating that the pentacoordinated form of the inhibitor is present to a much lesser degree than the octahedral form, probably around 5% or so of the total occupancy. Due to concerns with resolution, the pentacoordinated form has not been included in the current model and only an octahedral form is refined here.

DISCUSSION

Serine acyl hydrolases are susceptible to inhibition by vanadium (V)/hydroxamic acid complexes (*26*). Chymotrypsin, for example, forms a complex with vanadate and benzohydroxamic acid with a dissociation constant (referring to dissociation of a 1:1 vanadate/benzohydroxamate complex from the enzyme) of 16 μM. The inhibition appears to be competitive (Figures 2 and 3). Inhibition may occur, as with other examples of "enzyme-assembled" or "target-induced" inhibitors (*54−57*), either by stepwise binding of the ligands, vanadate and benzohydroxamic acid in this case, or by interaction with a preformed complex of the ligands in solution. Since vanadate and benzohydroxamic acid, individually, do not inhibit at the concentrations employed, and the 1:1 complex does occur in solution (*28*), the latter path is perhaps more likely in this case. The X-ray crystal structure of the inhibitory complex has now been determined; it has been described above and will be discussed below in terms of the catalytic mechanism and substrate specificity of chymotrypsin.

As described in the introduction, serine acyl hydrolases such as chymotrypsin catalyze the hydrolysis of carboxylic acid derivatives by means of a double displacement mechanism. After noncovalent binding of substrate to enzyme, the reaction is initiated by nucleophilic attack by the active site serine hydroxyl group on the acyl carbonyl group of the substrate, to form, initially, the tetrahedral intermediate **10**.
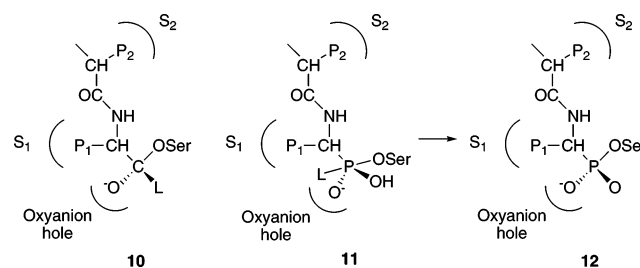
This structure shows the oxyanion hole (backbone NH groups of Gly 193 and Ser 195), the S_1 and S_2 subsites accommodating the P_1 and P_2 side chains of the substrate, and the leaving group L. A phosphonate inhibitor, designed to take advantage of chymotrypsin specificity (see, for example, ref *14*), would react by way of the pentacoordinated intermediate **11**. Again, L is a leaving group, but, as stereoelectronically required in a phosphyl transfer transition state (*16*), is in line with the SerOγ−P bond rather than adjacent as in **10**. After departure of L, **11** would, in principle, yield the acyl transfer transition state analogue structure **12**.
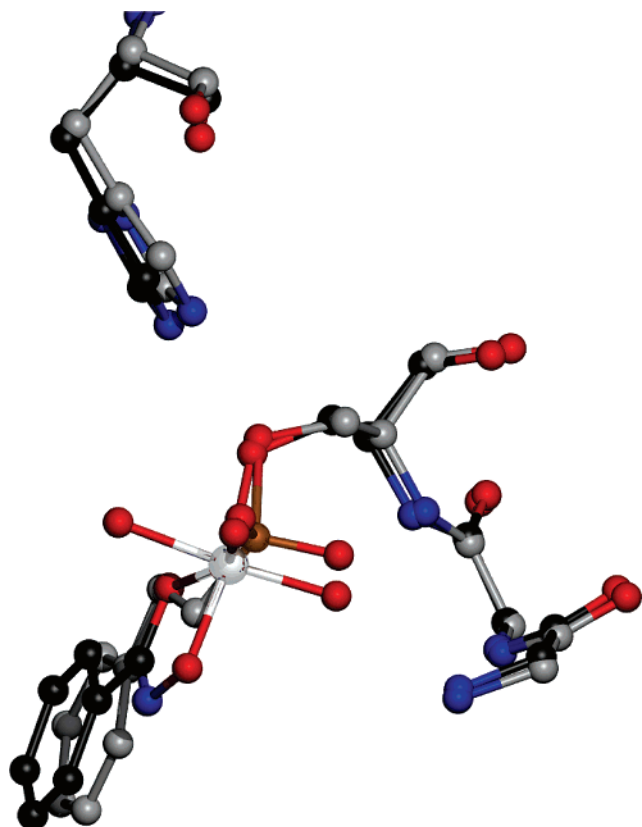
FIGURE 6: Overlapped structures showing the resemblance between the positioning of ligands in the vanadate complex and the phenylethane boronic acid complex (*44*). The vanadate/hydroxymate/γ-chymotrypsin complex is rendered with carbons in black and the vanadium ion in chrome. The phenylethane boronic acid/γ-chymotrypsin complex is rendered with carbons in gray and the boron in bronze. The side chain of histidine 57 is included for perspective as is the oxyanion hole consisting of the backbone amides from serines 193 and 195. Only side chains for His 57 and Ser 195 are rendered.

If the vanadate complex formed a direct analogue of **11**, one would expect the structure **13**. It is noticeable, however, that in **13**, neither the S_1 nor the S_2 sites appear to be optimally, or even suboptimally, filled [chymotrypsin has a preference for bulky aliphatic residues in S_2 (*58*)]. Further,

in complexes of peptide analogues with chymotrypsin, the $P_1 - P_2$ amide connector usually only interacts with the protein via a single hydrogen bond to Ser 214 (*42*, *59*). Thus it is perhaps not surprising, in retrospect, that the observed structure does not resemble **13**. In serine β-lactamases, where an aromatic side chain and an amide group of a substrate interact more favorably with the enzyme, the result may be different, although no structure is yet available to demonstrate this.

The observed structure must be represented as **14** rather than **13** but can be interpreted in terms of **11**. The chymotrypsin has bound the hydroxamate oxygen in a position roughly equivalent to that of the leaving group (L) in the pentacoordinated intermediate structure **11**. Then, by virtue
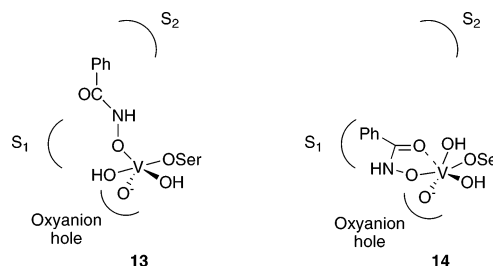
of the hydroxamate structure, the remainder of the ligand has become organized to place the phenyl group in the important S_1 site, and the carbonyl coordinated to the vanadium in a chelated fashion as found in small molecule complexes of vanadate and hydroxamic acids. The vanadium, perhaps because of the weak interaction with the hydroxamate carbonyl, has achieved coordination saturation by means of another hydroxyl/water ligand directed in the empty S_2 direction. The maneuvering of the phenyl group into the S_1 site can be appreciated in Figures 6 and 7 that show overlaps of the vanadate complex with structures of complexes of the acyl transfer transition state analogue phenylethane boronic acid (*44*) and of a peptide substrate in the acyl−enzyme form (*42*).

Overall, the ligands around vanadium in the observed structure form a distorted octahedron but, as indicated above, one can see in them an analogue of the pentacoordinated
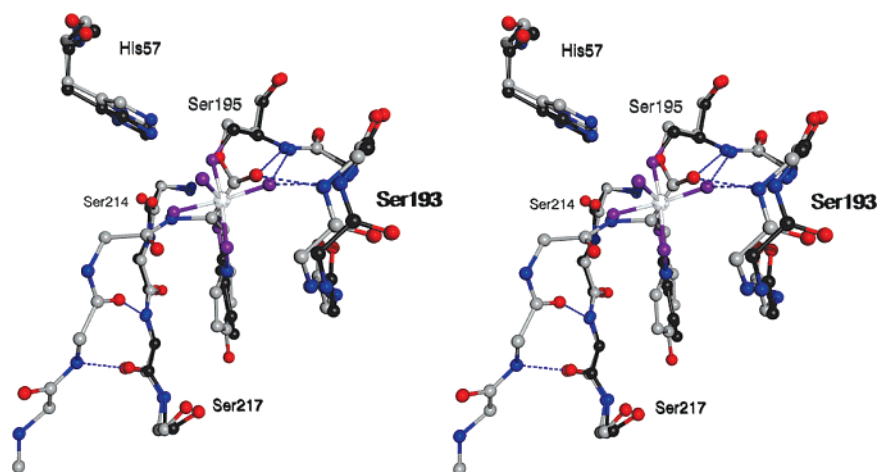

FIGURE 7: A wall-eyed stereoview of overlapped structures showing the resemblance between the positioning of ligands in the vanadate complex and a γ-chymotrypsin/peptide acyl enzyme (*43*). The vanadate/hydroxamate/γ-chymotrypsin complex is rendered with carbons in black, the vanadium ion in chrome, and the oxygens bonded to the vanadium ion in purple. The γ-chymotrypsin/peptide acyl enzyme is rendered with carbons in gray. Blue dashed lines represent pertinent hydrogen bonds. All side chains except those for histidine 57 and serine 195 and the P1 tyrosine of the peptide have been removed for clarity.

complex **11**; the latter, in this case, is unusual in having an extended leaving group enabling it to reach into the S_1 site. To some extent, the structure could also be seen as an analogue of a tetrahedral structure **10**, but the higher vanadium coordination seems to make it appear closer to **11**.

Other than by structural considerations, a semiquantitative estimate of the ability of the vanadate complex to mimic a chymotrypsin transition state may be obtained from the K_I value of the vanadate complex (14 μM). The corresponding values for two generally acknowledged small molecule sources of tetrahedral transition state analogues, phenylethane boronic acid (*44*) and *N*-acetyl-L-phenylanyl trifluoromethyl ketone (*60*), are 40 μM and 20 μM, respectively; small molecule substrates bind considerably more weakly (*61*). The vanadate complex, therefore, is a quite effective inhibitor and, perhaps, as discussed above, a phosphylation transition state analogue.

The structure obtained and described in this paper, the first of a vanadium inhibitor of an acyl transfer enzyme, does indicate that, as would be expected, an enzyme should be able to bind an analogue of a transition state of a catalyzed reaction, even if the reaction is not the one the enzyme has evolved to facilitate (Figure 1). This idea may expand the possibilities of inhibitor design, particularly for covalent inhibitors. In the present case, by analogy with other transition state analogue inhibitors of serine proteases (*58*, *60*, *61*), one might speculate that a peptide hydroxamate, designed for optimal occupancy of the S_2 rather than the S_1 site, e.g., an *N*-acyl-leucine hydroxamic acid, might form a tight binding vanadate complex resembling **13** with chymotrypsin. Unfortunately, peptide hydroxamates do not form as stable complexes with vanadium in solution as do aryl hydroxamates (*27*, *62*). Further, chymotrypsin specificity is dominated by the S_1 site; an enzyme with more significant extended specificity might be a better target for this approach. It is also intriguing to note that **14** has two remaining exchangeable oxygen sites at vanadium which could be displaced by enzyme-specific ligands.

ACKNOWLEDGMENT

REFERENCES

1. Baker, B. R. (1967) Design of active-site directed irreversible enzyme inhibitors, John Wiley, NY.
2. Pauling, L. (1948) Chemical achievement and hope for the future, *Am. Sci. 36*, 50−58.
3. Wolfenden, R. (1972) Analog approaches to the structure of the transition state in enzyme reactions, *Acc. Chem. Res. 5*, 10−18.
4. Lienhard, G. E. (1973) Enzymatic catalysis and transition-state theory, *Science 180*, 149−154.
5. Endo, K., Helmcamp, G. M., and Bloch, K. (1970) Mode of inhibition of β-hydroxydecanoyl thioester dehydrase by 3-decynoyl-N-acetylcysteamine, *J. Biol. Chem. 245*, 4293−4296.
6. Bloch, K. (1986) The beginnings of enzyme suicide, *J. Prot. Chem. 5*, 281−288.
7. Rando, R. R. (1975) Mechanisms of action of naturally occurring irreversible enzyme inhibitors, *Acc. Chem. Res. 8*, 281−288.
8. Abeles, R. H., and Maycock, A. L. (1976) Suicide enzyme inactivators, *Acc. Chem. Res. 9*, 313−319.
9. Bender, M. L. (1960) Mechanisms of catalysis of nucleophilic reactions of carboxylic acid derivatives, *Chem. Rev. 60*, 53−113.
10. Hartley, B. S. (1960) Proteolytic enzymes, *Annu. Rev. Biochem. 29*, 45−72.
11. Kraut, J. (1977) Serine proteases−structure and mechanism of catalysis, *Annu. Rev. Biochem. 46*, 331−358.
12. Dixon, G. H., Neurath, H., and Pechere, J. F. (1958) Proteolytic enzymes, *Annu. Rev. Biochem. 27*, 489−532.
13. Balls, A. K., and Jansen, E. F (1952) Stoichiometric inhibition of chymotrypsin, *Adv. Enzymol. 13*, 321−343.
14. Bartlett, P. A., and Lamden, L. A. (1986) Inhibition of chymotrypsin by phosphonate and phosphonamidate peptide analogs, *Bioorg. Chem. 14*, 356−377.
15. Oleksyszyn, J., and Powers, J. C. (1991) Irreversible inhibition of serine proteases by peptide derivatives of (α-aminoalkyl)-phosphonate diphenyl esters, *Biochemistry 30*, 485−493.
16. Westheimer, F. H. (1968) Pseudo-rotation in the hydrolysis of phosphate esters, *Acc. Chem. Res. 1*, 70−78.
17. Rahil, J., and Pratt, R. F. (1992) Mechanism of inhibition of the class C β-lactamase of *Enterobacter cloacae* P99 by phosphonate monoesters, *Biochemistry 31*, 5869−5878.
18. Lindquist, R. N., Lynn, J. L., Jr., and Lienhard, G. E. (1973) Possible transition-state analogs for ribonuclease. Complexes of uridine with oxovanadium(IV) ion and vanadium(V) ion, *J. Am. Chem. Soc. 95*, 8762−8768.
19. Gresser, M. J., and Tracey, A. S. (1990) in *Vanadium in Biological Systems. Physiology and Biochemistry* (Chasteen, N. D., Ed) Chapter IV, Kluwer Academic, Dordrecht, The Netherlands.
20. Stankiewcz, J. P., Tracey, A. S., and Crans, D. C. (1995) in *Metal Ions in Biological Systems, Vol. 31, Vanadium and its Role in Life* (Sigel, H., and Sigel, A., Eds.) Chapter 9, Marcel Dekker, New York.
21. Crans, D. C., Smee, J. J., Gaidamauskas, E., and Yang, L. (2004) The chemistry and biochemistry of vanadium and the biological activities exerted by vanadium compounds, *Chem. Rev. 104*, 849−902.
22. Wlodawer, A., Miller, M., and Sjolin, L. (1983) Active site of RNase: neutron diffraction study of a complex with uridine vanadate, a transition-state analog, *Proc. Natl. Acad. Sci. U.S.A. 80*, 3628−3631.
23. Lindqvist, Y., Schneider, G., and Vikho, P. (1994) Crystal-structures of rat acid-phosphatase complexed with the transition-state analogs vanadate and molybdate−implications for the reaction mechanism, *Eur. J. Biochem. 221*, 139−142.
24. Zhang, M., Zhou, M., Van Etten, R. L., and Stauffacher, C. V. (1997) Crystal structure of bovine low molecular weight phosphotyrosyl phosphatase complexed with the transition state analog vanadate, *Biochemistry 36*, 15−23.
25. Holtz, K. M., Stec, B., and Kantrowitz, E. R. (1999) A model of the transition state in the alkaline phosphatase reaction, *J. Biol. Chem. 274*, 8351−8354.
26. Bell, J. H., Curley, K., and Pratt, R. F. (2000) Inhibition of serine amidohydrolases by complexes of vanadate with hydroxamic acids, *Biochem. Biophys. Res. Commun. 274*, 732−735.
27. Bell, J. H., and Pratt, R. F. (2002) Mechanism of inhibition of the β-lactamase of *Enterobacter cloacae* P99 by 1:1 complexes of vanadate with hydroxamic acids, *Biochemistry 41*, 4329−4338.
28. Bell, J. H., and Pratt, R. F. (2002) Formation and structure of 1:1 complexes between aryl hydroxamic acids and vanadate at neutral pH, *Inorg. Chem. 41*, 2747−2753.
29. DelMar, E. G., Largman, C., Broderick, J. W., and Geokas, M. C. (1979) A sensitive new substrate for chymotrypsin, *Anal. Biochem. 99*, 316−320.
30. Kuzmic, P. (1996) Program DYNAFIT for the analysis of enzyme kinetic data: Application to HIV proteinase, *Anal. Biochem. 237*, 260−273.
31. Cleland, W. W. (1979) Statistical analysis of enzyme kinetic data, *Methods Enzymol. 63*, 103−138.
32. Merli, A., and Rossi, G. L. (1986) Deacylation kinetics of gamma-chymotrypsin in solution and in the crystal. *FEBS Lett. 199*, 179−81.
33. Dixon, M. M., and Matthews, B. W. (1989) Is γ-chymotrypsin a tetrapeptide acyl-enzyme adduct of α-chymotrypsin?, *Biochemistry 28*, 7033−7038.
34. Otwinowski, Z., and Minor, W. (1997) Processing of X-ray diffraction data collected in oscillation mode, *Methods Enzymol. 276*, 307−326.
35. Brunger, A. T., Adams, P. D., Clore, G. M., DeLano, W. L., Gros, P., Grosse-Kunstleve, R. W., Jiang, J. S., Kuszewski, J., Nilges, M., Pannu, N. S., Read, R. J., Rice, L. M., Simonson, T., and Warren, G. L. (1998) Crystallography & NMR system: A new

software suite for macromolecular structure determination, *Acta Crystallogr., Sect. D: Biol. Crystallogr. 54*, 905−921.

36. Cohen, G. H., Silverton, E. W., and Davies, D. R. (1981) Refined crystals structure of γ-chymotrypsin at 1.9 Å resolution, *J. Mol. Biol. 148*, 449−479.

37. Adams, P. D., Pannu, N. S., Read, R. J., and Brünger, A. T. (1997) Cross-validated maximum likelihood enhances crystallographic simulated annealing refinement, *Proc. Natl. Acad. Sci. U.S.A. 94*, 5018−5023.

38. Rice, L. M., and Brünger, A. T. (1994) Torsion angle dynamics: reduced variable conformational sampling enhances crystallographic structure refinement, *Proteins 19*, 277−290.

39. Jones, T. A., Zou, J. Y., Cowan, S. W., and Kjeldgaard, M. (1991) Improved methods for building protein models in electron density maps and the location of errors in these models, *Acta Crystallogr. A 47*, 110−119.

40. Sheldrick, G. M., and Schneider, T. R. (1997) SHELXL: High Resolution Refinement, *Methods Enzymol. 277*, Macromolecular Crystallography, Part B, 319−343.

41. Fisher, D. C., Barclay-Peet, S. J., Balfe, C. A., and Raymond, K. N. (1989) Synthesis and characterization of vanadium(V) and -(IV) hydroxamate complexes. X-ray crystal structures of oxochlorobis-(benzohydroxamato)vanadium(V) and oxoisopropoxo(N,N′-dihydroxy-N,N′-diisopropylheptanediamido)vanadium(V), *Inorg. Chem. 28*, 4399−4406.

42. Dixon, M. M., Brennan, R. G., and Matthews. B. W. (1991) Structure of γ-chymotrypsin in the range pH 2.0 to pH 10.5 suggests that γ-chymotrypsin is a covalent acyl-enzyme adduct at low pH, *Int. J. Biol. Macromol. 13*, 89−96.

43. Harris, T. K., and Mildvan, A. S. (1999) High-precision measurement of hydrogen bond lengths in proteins by nuclear magnetic resonance methods, *Proteins: Struct., Funct., Genet. 35*, 275−281.

44. Tulinsky, A., and Blevins, R. A. (1987) Structure of a tetrahedral transition state complex of γ-chymotrypsin dimer at 1.8 Å resolution, *J. Biol. Chem. 262*, 7737−7743.

45. Pecoraro, V. L. (1989) Structural characterization of [VO-(salicylhydroximate)(CH3OH)]3: applications to the biological chemistry of vanadium(V). *Inorg. Chim. Acta 155*, 171−173.

46. Cornman, C. R., Colpas, G. J., Hoeschele, J. D., Kampf, J., and Pecoraro, V. L. (1992) Implications for the spectroscopic assignment of vanadium biomolecules: structural and spectroscopic characterization of monooxovanadium(V) complexes containing catecholate and hydroximate based noninnocent ligands, *J. Am. Chem. Soc. 114*, 9925−9933.

47. Gao, S., Weng, Z-Q., and Liu, S.-X. (1998) Syntheses and characterization of four novel monooxovanadium(V) hydrazone complexes with hydroxamate or alkoxide ligand, *Polyhedron 17*, 3595−3606.

48. Liu, S-X., and Gao, S. (1998) Synthesis and characterization of two novel monooxovanadium(V) complexes with bidentate benzohydroxamate ligand, *Inorg. Chim. Acta 282*, 149−154.

49. Chen, W., Gao, S., and Liu, S.-X. (1999) Monooxovanadium(V) complexes with bidentate N-phenylbenzohydroxamate, *Acta Crystallogr., Sect. C: Cryst. Struct. Commun. C55*, 531−533.

50. Yang, P., Han, G.-Y., Jin, X.-L., and Chen, S.-R. (2002) Synthesis, crystal structure and ab initio study of bis(benzohydroxamato)-oxo(isopropoxo)-vanadium(V), *Huaxue Xuebao 60*, 1072−1077.

51. Gao, S., Huo, L. H., Zhao, H., and Ng, S. W. (2004) (N-Benzoyl-N-phenylhydroxaminato-k2O,O′)(salicylaldehyde isonicotinoyl-hydrazonato-k3O,N,N′)vanadium(IV) hexane hemisolvate, *Acta Crystallogr., Sect. E: Struct. Rep. Online E60*, m1757−m1758.

52. Larsen, I. K. (1971) Crystal and molecular structures of syn-ethyl and anti-ethyl benzohydroximate, *Acta Chem. Scand. 25*, 2409−2420.

53. Maurya, M. R., Agarwal, S., Bader, C., Ebel, M., and Rehder. D. (2005) Synthesis, characterisation and catalytic potential of hydrazonato-vanadium(V) model complexes with [VO]3+ and [VO2]+ cores, *Dalton Trans.* 537−544.

54. Katz, B. A., Finer-Moore, J., Mortezaei, R., Rich, D. H., and Stroud, R. M. (1995) Episelection: novel K_i ~ nanomolar inhibitors of serine proteases selected by binding or chemistry on an enzyme surface, *Biochemistry 34*, 8264−8280.

55. Suenaga, H., Yamamoto, H., and Shinkai, S. (1996) Screening of boronic acids for strong inhibition of the hydrolytic activity of α-chymotrypsin and for sugar sensing associated with a large fluorescence change, *Pure Appl. Chem. 68*, 2179−2186.

56. Tian, Z.-Q., Brown, B. B., Mack, D. P., Hutton, C. A., and Bartlett, P. A. (1997) Potentially Macrocyclic Peptidyl Boronic Acids as Chymotrypsin Inhibitors, *J. Org. Chem. 62*, 514−522.

57. Transue, T. R., Krahn, J. M., Gabel, S. A., DeRose, E. F., and London, R. E. (2004) X-ray and NMR characterization of covalent complexes of trypsin, borate, and alcohols, *Biochemistry 43*, 2829−2839.

58. Kurachi, K., Powers, J. C., and Wilcox, P. E. (1973) Kinetics of the reaction of chymotrypsin Aα with peptide chloromethylketones in relation to its substrate specificity, *Biochemistry 12*, 771−777.

59. Brady, K., Wei, A., Ringe, D., and Abeles, R. H. (1990) Structure of chymotrypsin−trifluoromethylketone inhibitor complexes: comparison of slowly and rapidly equilibrating inhibitors, *Biochemistry 29*, 7600−7606.

60. Imperiali, B., and Abeles, R. H. (1986) Inhibition of serine proteases by peptidyl fluoromethyl ketones, *Biochemistry 25*, 3760−3767.

61. Kettner, C. A., Bone, R., Agard, D. A., and Bachovchin, W. W. (1988) Kinetic properties of the binding of α-lytic protease to peptide boronic acids, *Biochemistry 27*, 7682−7688.

62. Yamaki, R. T., Paniago, E. B., Carvalho, S., and Lula, J. S. (1999) Interaction of 2-amino-N-hydroxypropanamide with vanadium-(V) in aqueous solution, *J. Chem. Soc., Dalton. Trans.* 4407−4412.

63. Fenn, T. D., Ringe, D., and Petsko, G. A. (2003) POVScript+: a program for model and data visualization using persistence of vision ray-tracing, *J. Appl. Crystallogr. 36*, 944−947.

BI6025209